Pharmaceutical Sciences and Drug Design
ISSN: 3062-4428
2024, Volume 4, Page No: 197-211

Available online at: www.galaxypub.co/page/journals

Galaxy Publication

Galaxy Publication

Indirect ^18F-Labeling of Estradiol via Automated Click Chemistry: Radiochemical Development and In Vitro Evaluation

Ayesha Khan[1]*, Neha Patel[1], Rahul Verma[1]

[1]Department of Pharmaceutical Sciences, Faculty of Pharmacy, University of Delhi, Delhi, India.

***E-mail** ✉ ayesha.khan@outlook.com

Received: 29 January 2024; **Revised:** 07 April 2024; **Accepted:** 12 April 2024

ABSTRACT

Click chemistry provides a powerful method for selectively linking diverse molecular building blocks to create sophisticated molecules efficiently. Here, we report the use of copper(I)-catalyzed biorthogonal cycloaddition between alkynes and azides for the indirect incorporation of fluorine-18 into an estradiol-based compound, aimed at imaging estrogen receptors. The synthesis protocol was entirely established and refined using an automated module, with parameters adjusted to deliver the target molecule in satisfactory yield and avoid any solid formation. While the in vitro and in vivo data did not support advancement as a clinical radiotracer, the results are nonetheless important because automated systems are indispensable for producing PET tracers reliably and repeatedly under Good Manufacturing Practice standards, all while reducing radiation exposure to staff.

Keywords: 18F labeling, Breast cancer imaging, Click chemistry, Radiochemical development

How to Cite This Article: Khan A, Patel N, Verma R. Indirect ^18F-Labeling of Estradiol via Automated Click Chemistry: Radiochemical Development and In Vitro Evaluation. Pharm Sci Drug Des. 2024;4:197-211. https://doi.org/10.51847/MiQjUEL35m

Introduction

Click chemistry encompasses a family of reactions noted for their excellent yields and specificity, permitting the efficient connection of two molecular fragments with byproducts that are simple to eliminate under benign reaction conditions. This approach was originally conceptualized by the laboratory of Dr. Barry Sharpless [1] and has since been broadly adopted in areas like pharmaceutical development, biological ligation, polymer chemistry, and nanotechnology [2-4]. Radiopharmaceutical design has similarly benefited from these reactions [5, 6]. The initial example in this area involved forming triazole-containing polydentate chelators bound to peptides or proteins through the classic Huisgen 1,3-dipolar cycloaddition of terminal alkynes with organic azides [7]. Notably, 1,4-substituted 1,2,3-triazoles function as flexible coordinating agents with multiple binding sites for transition metals and have seen extensive use in designing candidate 99mTc-based imaging agents [8-10]. Our laboratory has leveraged this technique to generate technetium-labeled conjugates of glucose, nitroimidazole, flutamide, and estradiol analogs **(Figure 1)** [11-16].

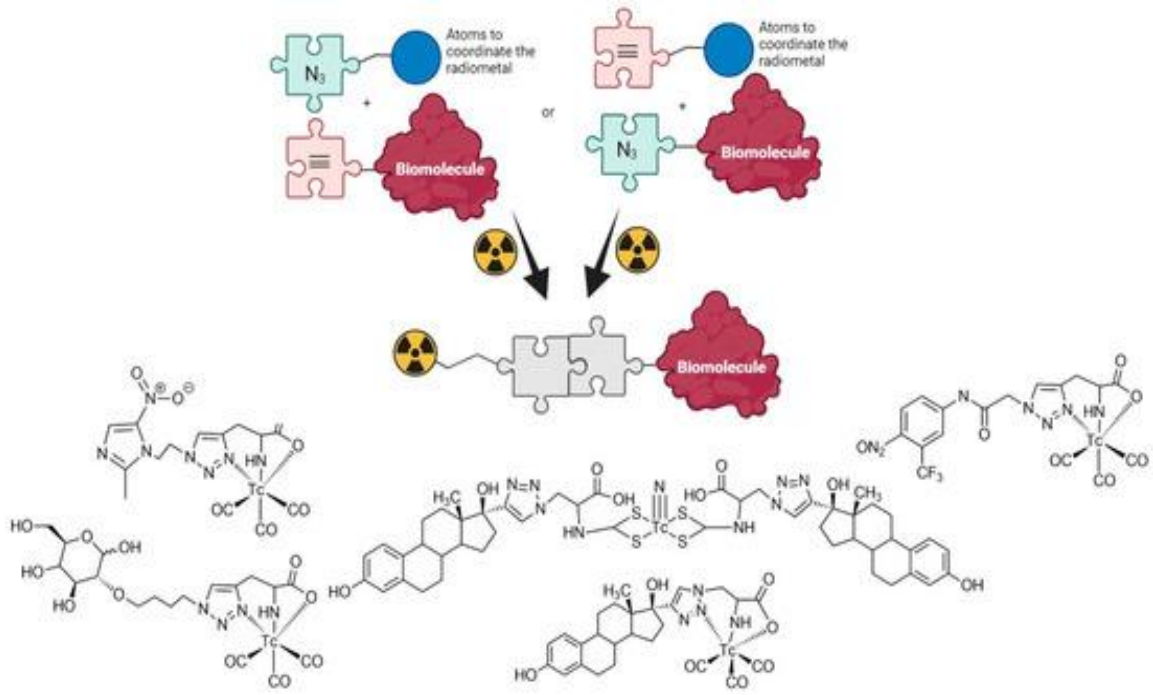

Figure 1. 99mTc complexes with different biomolecules synthesized by our group using "click reactions".

A further prominent role for click chemistry in radiopharmaceuticals lies in building labeling precursors by appending prosthetic moieties for radiohalogen introduction [17, 18]. Among positron-emitting isotopes, fluorine-18 stands out as the most common choice for PET due to its suitable decay properties (half-life of 109.7 min and positron energy of 635 keV) and rich organic chemistry that supports both nucleophilic and electrophilic pathways for direct 18F attachment to many compounds of interest. That said, the demanding conditions of direct fluorination often damage sensitive biological molecules. Indirect strategies—first preparing a radiolabeled synthon and then conjugating it—offer a gentler alternative that preserves biomolecule integrity by bypassing extreme pH or heat [19, 20].

The current study outlines the implementation of Huisgen cycloaddition to produce [18F]F-FEET **(Figure 2)**, a modified estradiol intended for PET visualization of estrogen receptors (ER). Estrogen receptors are nuclear hormone receptors central to breast cancer pathophysiology. They appear in merely 6–10% of healthy mammary epithelial cells but are overexpressed in approximately 70% of initial breast malignancies. Tumors classified as ER-positive (ER+) typically show good response to endocrine therapy, whereas ER-negative (ER−) cases demand different therapeutic approaches [21-24]. Reliable detection of ER status in tumors serves as a key prognostic marker and helps forecast likely benefit from hormone-blocking treatments. Biopsy remains a standard technique for this assessment, yet tumor heterogeneity means a tiny sample might not capture the full receptor profile. Additionally, the procedure is invasive, entails risks, can be uncomfortable for patients, may disturb the local tumor environment, and could fail to sample relevant areas [23, 24]. Nuclear medicine-based molecular imaging complements biopsy effectively, being far less invasive, enabling repeated measurements over time, supplying functional rather than just anatomical data, and surveying large or whole-body regions [25]. From the 1980s onward, various teams have tested both steroid-derived and non-steroid ligands as PET or SPECT probes for ER visualization in breast cancer cases, though the majority faltered during animal testing or initial human trials. A landmark achievement came in 1984 when Kiesewetter and colleagues [26] introduced 16α-[18F]fluoroestradiol ([18F]FES) [21, 26, 27]. Subsequent work confirmed that [18F]FES detects tracer accumulation in both primary lesions and metastases with high sensitivity and aids in tracking treatment response to hormone therapy. Limitations persist, however, particularly the inability to identify hepatic metastases because of substantial background from physiological tracer clearance in the liver [22, 25, 28-31]. In May 2020, the U.S. FDA authorized [18F]FES for PET imaging to identify estrogen receptor-positive sites and to supplement biopsy findings in individuals with relapsed or metastatic breast cancer [32]. Even with this milestone, ongoing efforts to devise superior ER-directed radiotracers that overcome the drawbacks of [18F]FES are strongly warranted.

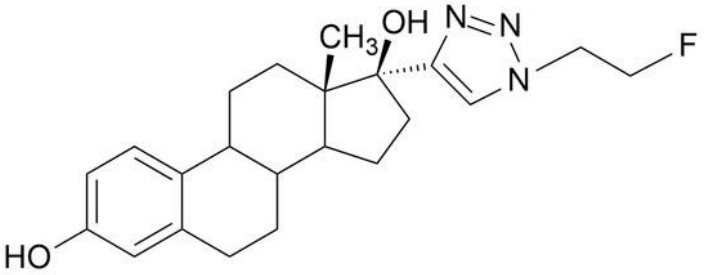

Figure 2. Structure of [18F]F-FEET.

The compound [18F]F-FEET, chemically named (13S,17S)-17-(1-([18F]2-fluoroethyl)-1H-1,2,3-triazol-4-yl)-13-methyl-7,8,9,11,12,13,14,15,16,17-decahydro-6H-cyclopentaphenanthrene-3,17-diol, exhibits the standard pharmacophore features required for an estrogen receptor agonist, such as an aromatic A-ring and hydrogen-bonding hydroxyl groups at positions C3 and C17. The distance between the oxygen atoms of these two hydroxyl groups is exactly 11 Å, supported by a rigid hydrophobic core; these structural elements are essential for maintaining biological activity [33, 34]. Radiofluorination was performed indirectly by attaching a prosthetic group at the 17-position of ethinylestradiol via a triazole formed through click chemistry, with a two-carbon linker bearing the [18F]fluorine atom connected to the 4-position of the triazole **(Figure 2).**

Materials and Methods

General

Reagents were analytical purity and applied directly without extra refining. Thin-layer chromatography (TLC) utilized ready-coated silica plates (Sigma Aldrich, Merck Group, San Luis, MI, USA) and standard anisaldehyde for spot detection. Proton NMR data were acquired at 400 MHz using $CDCl_2$ as solvent, with shifts (δ) in ppm referenced to solvent residuals. Peak patterns are labeled s (singlet), d (doublet), t (triplet), or m (multiplet). Reactions employed dry solvents; analyses used HPLC-purity ones. Compound separation and detection occurred on a Shimadzu UFLC Prominence unit with SPD-M20A diode-array UV module (Shimadzu, Japan) plus B-FC-3200 gamma scintillation probe (LAB LOGIC). Columns were Phenomenex Phenosphere ODS (80 Å, 250 × 4.6 mm, 5 µm particle), eluted with water (A)/acetonitrile (B) gradient: 10–90% B (0–10 min), then isocratic 90% B (10–15 min) at 1.5 mL/min, tracking UV at 280 nm and radioactivity. Software control was via LabSolutions® v5.9. Activity readings came from a Capintec CRC 25 calibrator. In vitro and physicochemical counts used an ORTEC digiBASE multichannel NaI(Tl) detector (2.5 × 2.5 inch crystal, 1086 channels).

Synthesis

Synthesis of A

2-Bromoethanol (1.34 g, 10.95 mmol) and NaN_3 (0.85 g, 13.14 mmol) were dissolved in dry DMSO (30 mL), heated under N_2 at 100 °C for 6 h, then left stirring at ambient temperature for another 18 h. Solvent was stripped at reduced pressure (60 °C), followed by ether/water partitioning (10 × 10 mL each). Organics were $MgSO_4$-dried, concentrated at 25 °C under vacuum, delivering A (yellow oil, 90% yield).

^{1}H NMR A (400 MHz, $CDCl_3$) δ (ppm): 3.76 (m, 2H), 3.38 (t, 2H).

Synthesis of B

Crude A (0.87 g, 9.99 mmol) in dry CH_2Cl_2 (30 mL) plus Et_3N (2 mL, 6.46 mmol) was iced to 0 °C before slow addition of mesyl chloride in CH_2Cl_2 (2.26 g, 11.90 mmol). Warming to room temperature, the N_2-protected stir continued 5 days. Alumina column elution with hexane/EtOAc (7:3) purified B (yellow oil, 17% yield).

^{1}H NMR B (400 MHz, $CDCl_3$) δ (ppm): 7.83 (d, 2H), 7.38 (d, 2H), 4.17 (t, 2H), 3.49 (t, 2H), 2.46 (s, 3H).

Synthesis of C

B (0.66 g, 2.73 mmol) and ethinylestradiol (0.40 g, 1.36 mmol) in t-BuOH (6 mL) received an aqueous mix of ascorbic acid (0.011 g, 0.055 mmol) and $Cu(OAc)_2$ (0.020 g, 0.11 mmol) (4 mL water). Stirring proceeded 6 days at room temperature, dark, under N_2. EtOAc extractions (10 × 10 mL), $MgSO_4$ drying, and vacuum removal at 40 °C gave crude C (yellow oil, apparent yield >100%).

^{1}H NMR C (400 MHz, $CDCl_3$) δ (ppm): 7.69 (d, 2H), 7.52 (s, 1H), 7.31 (d, 2H), 7.17 (d, 1H), 7.06 (d, 1H), 6.65 (dd, 1H), 6.62 (dd, 1H), 6.57 (d, 1H), 6.55 (d, 1H), 4.66 (t, 2H), 4.42 (t, 2H), 2.80 (m, 4H), 2.61 (s, 1H), 2.40–1.25 (m, 20H), 1.05 (s, 3H), 0.88 (s, 6H).

Synthesis of [19F]F-FEET

Compound C (0.05 g, 0.09 mmol) was combined with tetrabutylammonium fluoride (TBAF) (0.030 g, 0.11 mmol) in dry DMF (2.5 mL). Heating proceeded at 130 °C for 6 h under nitrogen and away from light. Workup involved multiple ether/water extractions (10 × 10 mL), followed by vacuum concentration at 60 °C, yielding a yellow oil (39.6%).

MS (EI, 10 eV) m/z: 385 (M^+).

Radiolabeling

Production of [18F]F$^-$

Highly enriched [18O]H_2O (>98%, Huayi Isotopes) was irradiated in a GE PETtrace cyclotron target using 16 MeV protons, producing 18.5–55.5 GBq (18,500–55,500 MBq) of no-carrier-added [18F]fluoride via the $^{18}O(p,n)^{18}F$ reaction. The activity was then routed to the Synthra RNplus Research synthesizer.

Conditioning of 18F

Aqueous [18F]fluoride was trapped on a Sep-Pak® QMA Light cartridge (Waters, Germany). Release into the reaction vessel was achieved with K_2CO_3 (3.5 mg) and Kryptofix 2.2.2 (Sigma Aldrich, San Luis, MI, USA) (15 mg) in 1:9 H_2O/MeCN (1000 µL). Traces of water were eliminated by heating at 95 °C under helium flow and vacuum.

Radiofluorination of C to obtain [18F]F-FEET

To the dried [18F]fluoride residue was added precursor C (1 mg, 0.002 mmol) in anhydrous acetonitrile (1 mL). The substitution reaction was maintained at 90 °C for 20 min.

Radiofluorination of B to obtain D

Activated [18F]fluoride (1850–5550 MBq) received precursor B (2 mg, 0.008 mmol) dissolved in dry acetonitrile (1 mL). Heating at 90 °C was applied for 20 min to effect labeling.

Complete synthesis of [18F]F-FEET in an automated module

Starting activity (3330–3700 MBq) of dry [18F]fluoride was treated with B (2 mg, 0.008 mmol) in dry MeCN (1 mL) at 90 °C for 20 min in the first reactor. The crude intermediate was then shuttled to reactor 2, where ethinylestradiol (0.001 mmol, 2 eq), 0.45 M $CuSO_4$ (0.01 mmol, 30 eq), 1.5 M sodium ascorbate (0.05 mmol, 100 eq) in methanol (300 µL), and 50 mM phosphate buffer pH 6 (100 µL) were introduced. Cycloaddition occurred at 80 °C for 30 min. Crude product underwent on-module purification via Sep-Pak® C18 Plus light cartridge (Waters, Germany).

Specific Activity = 0.22–0.25 GBq/µmol.

Physicochemical studies

Stability in the Labeling Milieu

The final radiotracer formulation was stored at room temperature. Samples taken at 1, 2, 3, and 4 h post-preparation were analyzed for radiochemical purity using the HPLC method described in Section 4.1.

Stability in human plasma

A portion of the radiotracer (100 µL, 47–53 MBq) was mixed with human plasma (1000 µL) and kept at 37 °C. At 1, 2, 3, and 4 h intervals, 200 µL portions were taken. Cold absolute ethanol (200 µL, −15 °C) was added to denature proteins, and the tubes were held at −20 °C for 5 min. Samples were then spun at 100× g for 5 min at 0 °C. Radiochemical purity of the clear supernatant was evaluated by HPLC according to the protocol in Section 4.1.

Lipophilicity

Hydrophobicity was measured at pH 7.4 as the octanol/phosphate buffer distribution coefficient (log Po/aq). In a tube, octanol (2 mL) and 0.1 M phosphate buffer pH 7.4 (1.9 mL) were equilibrated. Radiotracer (100 µL, 47–53 MBq) was introduced, the mixture vortexed vigorously for 2 min, and centrifuged (4000 rpm, 5 min). Duplicate 100 µL samples from each layer were withdrawn, and radioactivity counted on a solid scintillation detector. The experiment was repeated three times. Log Po/aq was computed as the ratio of counts in the organic layer to counts in the aqueous layer.

Plasma protein binding

Binding to plasma proteins (PPB) was quantified via size-exclusion on Illustra MicroSpin G-50 columns (GE Healthcare, Chicago, IL, USA). Control tubes contained 475 µL water + 25 µL tracer; test tubes had 475 µL human plasma + 25 µL tracer (12–14 MBq). Both were warmed at 37 °C for 30 or 60 min. Column preservative was cleared by spinning 1 min at 716× g. Then, 25 µL of control or test solution was applied and centrifuged 1 min at 716× g. Activity in the flow-through (bound fraction) and column retentate was measured by scintillation counting. Bound percentage was taken as activity in the eluate.

In vitro studies

Cellular experiments utilized the MCF-7 line (ATCC® HTB-22™, Manassas, VA, USA), an adherent human breast adenocarcinoma model. Cultures were maintained in T-75 flasks (Greiner Bio-One, Sigma Aldrich, Merck Group, San Luis, MI, USA) in DMEM (A1316, 9050 PanReac AppliChem ITW Reagents, Darmstadt, Germany) containing 10% fetal bovine serum (Gibco, ThermoFisher Scientific, Waltham, MA, USA), penicillin (100 U mL^{-1}, Sigma Aldrich, Merck Group, San Luis, MI, USA), and streptomycin (100 µg mL^{-1}, Sigma Aldrich, Merck Group, San Luis, MI, USA) under 37 °C and 5% CO_2.

Uptake assay dependent on the activity of the radiotracer

Confluent cultures (1 × 10^6 cells/T-75 flask) received [18F]F-FEET at 0.37, 0.74, 1.85, or 3.7 MBq and were incubated 1 h at 37 °C in 5% CO_2. Medium was then discarded, monolayers rinsed twice with PBS (10 mL), and cells released by trypsin-EDTA treatment (3 mL, 5 min, 37 °C, 5% CO_2). Radioactivity in detached cells and supernatant was quantified by scintillation counting. Cell-associated activity was reported as percentage of total.

Uptake assay dependent on the time of incubation

Confluent cultures (1 × 10^6 cells/T-75 flask) were exposed to 0.74 MBq [18F]F-FEET for 30 min, 1 h, or 2 h at 37 °C under 5% CO_2. Medium was removed, cells washed twice with PBS (10 mL), and harvested via trypsin-EDTA (3 mL, 5 min, 37 °C, 5% CO_2). Activity was counted separately in the pooled washes plus medium (12 mL + 20 mL PBS) and in the cell fraction using scintillation detection. Uptake was expressed as percentage of total activity in cells.

Results and Discussion

The radiotracer [18F]F-FEET was prepared using two distinct approaches. Method 1 employs precursor C, which features the estradiol scaffold and a tosylate leaving group to enable direct nucleophilic radiofluorination. Method 2 utilizes prosthetic group B, containing both a tosylate leaving group and an azide functionality, allowing milder conjugation to the pharmacophore via Huisgen cycloaddition with ethinylestradiol. Both routes are illustrated in **Figure 3.**

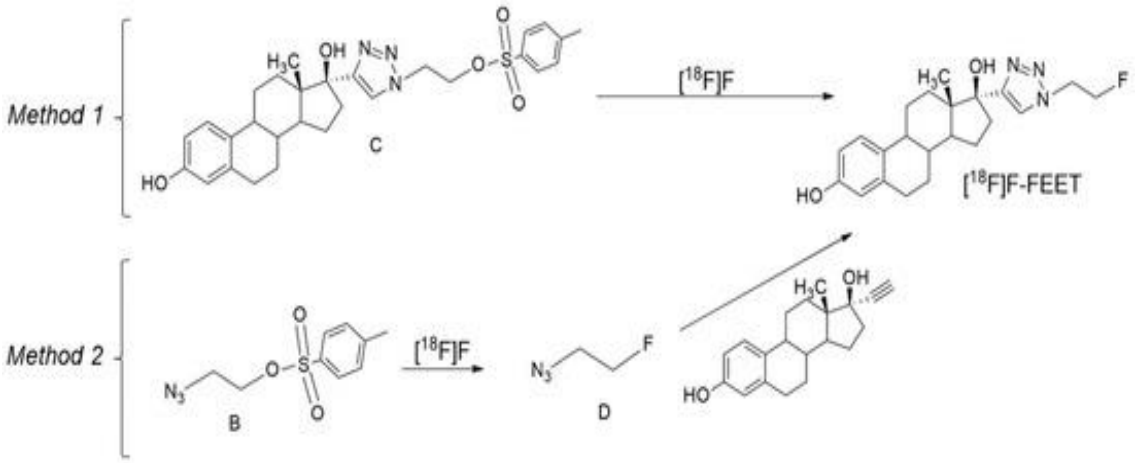

Figure 3. Synthesis of [18F]F-FEET by methods 1 and 2.

The non-radioactive reference compound FEET ([19F]F-FEET) was prepared to verify the identity of the radiolabeled product by co-elution in HPLC analysis. [19F]FEET was obtained by direct fluorination of compound C with tetrabutylammonium fluoride in DMF following a reported protocol [35]. The isolated product was purified and its structure confirmed using spectroscopic techniques.

Synthesis of [18F]F-FEET – method 1

Synthesis of C (Precursor)

Precursor C, 2-(4-((13S,17S)-3,17-dihydroxy-13-methyl-7,8,9,11,12,13,14,15,16,17-decahydro-6H-cyclopenta[a]phenanthren-17-yl)-1H-1,2,3-triazol-1-yl)ethyl 4-methylbenzenesulfonate, was synthesized in multiple steps starting from 2-bromoethanol as depicted in **Figure 4.** The sequence began with replacement of bromine by azide to yield intermediate A, followed by introduction of the tosylate to form B, and concluded with a Huisgen cycloaddition between the azide of B and the alkyne of ethinylestradiol to produce C **(Figure 4).**

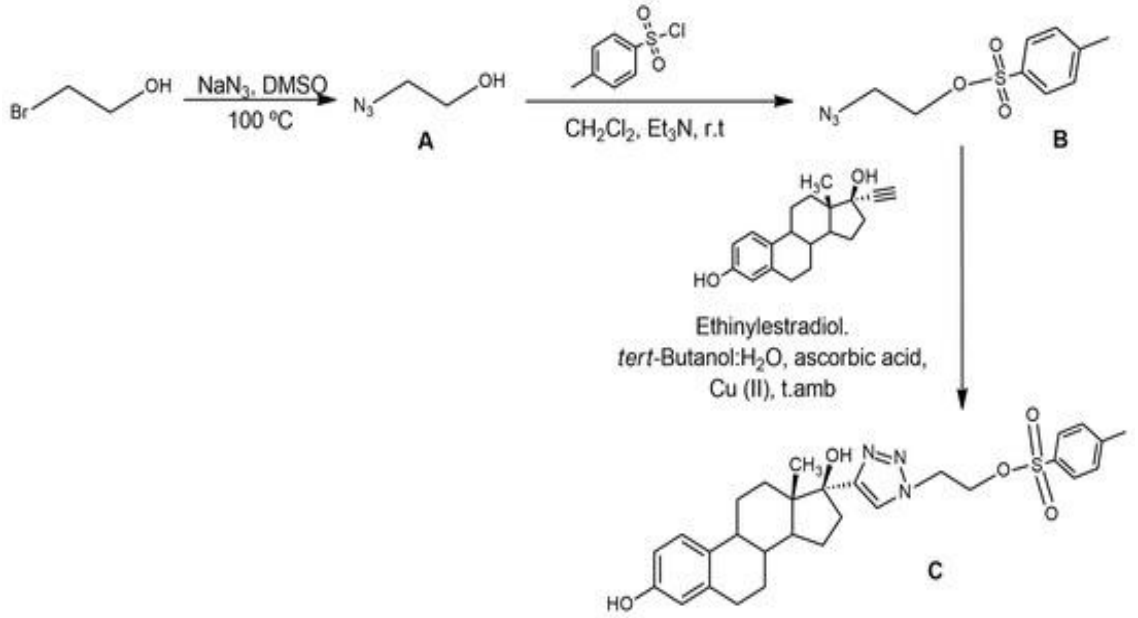

Figure 4. Synthesis of precursor (C).

Azide displacement of bromide was accomplished with sodium azide in dry dimethyl sulfoxide over 24 h according to the procedure of Berta *et al*. [36], affording A in over 90% yield. Tosylation was conducted using the method of Hay *et al*. [37]. Although mesyl chloride was not fully consumed after five days, the reaction was stopped upon detection of a new lower-Rf product by TLC. Purification on alumina column chromatography provided B in 17% yield. The final click cycloaddition was a Cu(I)-catalyzed 3+2 reaction between

ethinylestradiol's terminal alkyne and the azide of B, forming the triazole linkage. Cu(I) was generated in situ from Cu(II) and ascorbic acid in aqueous media [7, 13, 14]. After six days, ethyl acetate extraction yielded crude C with an apparent yield exceeding 100% due to contamination by residual ethinylestradiol and salts.

Radiofluorination of C to obtain [18F]F-FEET

Radiofluorination of precursor C was conducted via nucleophilic substitution on a Synthra RNplus Research automated module. Precursor C in DMSO was treated with Kryptofix® (Sigma Aldrich, San Luis, MI, USA) and K2CO3 at 50 °C for 30 min [35, 38]. Reaction progress was tracked by radio-HPLC. The gamma-detected chromatogram revealed substantial unreacted [18F]fluoride (retention time 1.4 min) and only 1.6% (ndc) of the desired product at 9.9 min, identified as [18F]F-FEET by co-injection with the non-radioactive standard (**Figures 5a and 5b).**

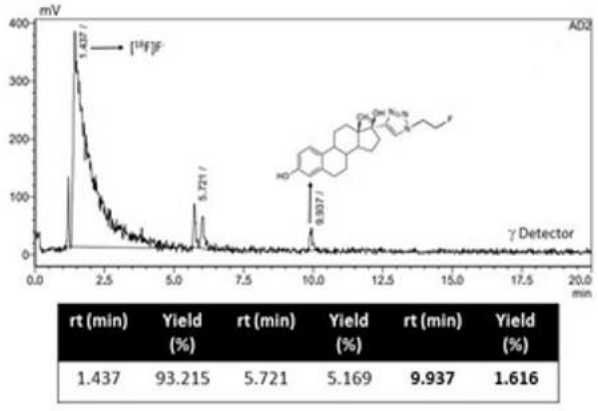

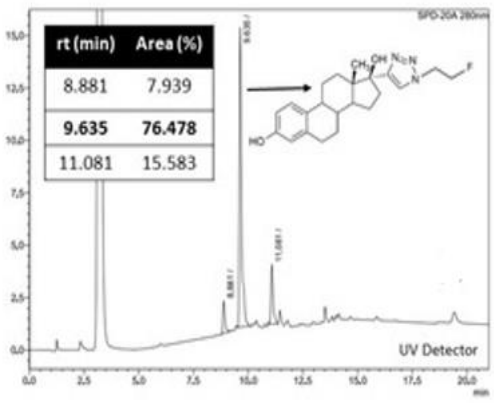

a) b)

Figure 5. (a) γ chromatographic profile obtained in the radiofluorination of C, (b) UV chromatographic profile obtained with [19F]F-FEET.

UV monitoring at 280 nm of the same reaction showed extensive decomposition of precursor C, with multiple new peaks and only a minor signal matching authentic C at 11 min **(Figures 6a and 6b).** The poor radiochemical yield was attributed to precursor instability under the demanding conditions of direct radiofluorination, prompting a shift to Method 2.

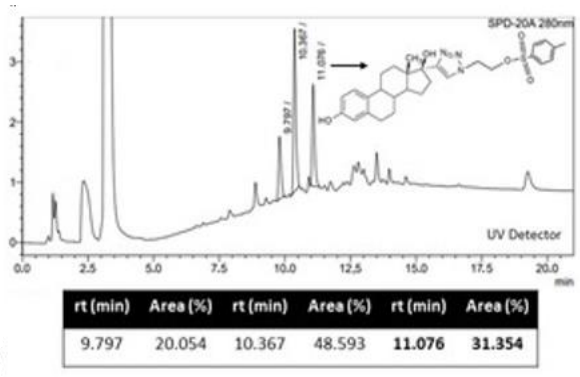

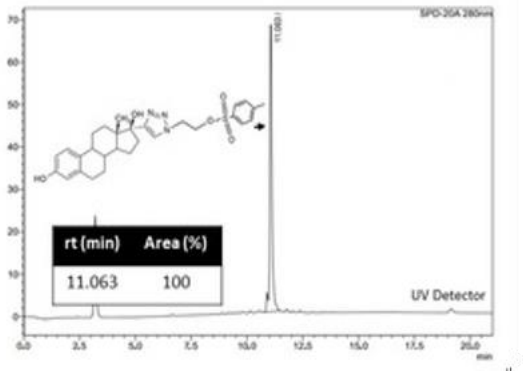

a) b)

Figure 6. (a) UV chromatographic profile obtained in the radiofluorination of C, (b) UV chromatographic profile of purified C.

Synthesis of [18F]F-FEET – method 2

Radiofluorination of B to obtain D

Method 2 involved initial nucleophilic radiofluorination of 2-azidoethyl 4-methylbenzenesulfonate (B), bearing a tosylate leaving group, to produce 1-azido-2-[18F]fluoroethane (D). The retained azide then enabled subsequent attachment of the biomolecule via Huisgen cycloaddition **(Figure 3)**—(Method 2).

Radiofluorination of B was executed on the Synthra RNplus Research module at 90 °C for 20 min using Kryptofix (Sigma Aldrich, San Luis, MI, USA) and K2CO3, conditions informed by literature and prior laboratory experience [35, 38]. Optimal radiochemical yields exceeding 90% (ndc) required 2 mg of B; reducing the amount to 1 mg lowered the yield to 69% (ndc).

Manual synthesis of [18F]F-FEET

With radiolabeled prosthetic group D secured in high yield (>90%, ndc), conjugation to ethinylestradiol was performed manually via click chemistry to furnish the target radiotracer. Starting conditions were adapted from published reports (Hausner *et al*. [39], Marik *et al*. [40], and Evans *et al*. [41]).

An initial 10:1 ethinylestradiol/D molar ratio with a 3:1 ethinylestradiol/CuI ratio and excess sodium ascorbate and base produced the product in 31% yield (ndc) after 10 min at room temperature. Extending the reaction time progressively raised the yield to 99% (ndc) **(Table 1)** (entries 1, 2, and 3). However, precipitation occurred under these conditions, hindering automation. To mitigate this, the amount of poorly soluble ethinylestradiol was decreased, and the temperature was raised to improve solubility. A 5:1 ethinylestradiol/D ratio at 80 °C for 15 min gave 69% yield (ndc) **(Table 1)** (entry 4), while extending to 30 min achieved 94% (ndc) **(Table 1)** (entry 5). Precipitation persisted in these trials.

Table 1. Optimization of Huisgen reaction's conditions using CuI as catalyst.

Experiment No.	Ethinylestradiol (equiv)	Ascorbic Acid (equiv)	CuI (equiv)	DIPEA (equiv)	D (equiv)	Reaction Time (min)	Reaction Temperature	Isolated Yield (%)
1	0.1	1	31	3	31	10	r.t	31.1
2	0.1	1	31	3	31	45	r.t	81.2
3	0.1	1	31	3	31	65	r.t	98.7
4	0.1	0.5	31	3	31	15	80 °C	69.3
5	0.1	0.5	31	3	31	30	80 °C	94.0
6	0.03	1	10	1	10	30	r.t	84.8
7	1	1.6	-	1.2	3.6	20	60 °C	4.2
8	1	1.6	-	1.2	3.6	30	60 °C	3.9

eq = equivalents, r.t = room temperature. Observations: Precipitation occurred under all tested reaction conditions.

Further experiments involved raising the equivalents of D while lowering those of Cu(I), sodium ascorbate, and base (**Table 1**, entries 6, 7, and 8). Satisfactory yields were obtained (Table 1, entry 6), yet precipitation was still observed in every trial.

Despite achieving acceptable radiofluorination yields, the persistent precipitate prompted a switch to more soluble catalytic systems, following the approach described by Glaser *et al*. [42], which employs Cu(II) as $CuSO_4$. Methanol was chosen as the solvent, with all reactions conducted at 80 °C while varying reagent equivalents and reaction durations **(Table 2).** An initial trial using a 6:1 ethinylestradiol/D molar ratio, 9 eq. of $CuSO_4$, 30 eq. of sodium ascorbate, and 15 min reaction time yielded only 6% (ndc) **(Table 2)**, (entry 1). Increasing $CuSO_4$ to 30 eq. and sodium ascorbate to 300 eq., while keeping ethinylestradiol and D masses unchanged, raised the yield to 55% (ndc) **(Table 2),** (entry 2). Extending the reaction time to 30 min further improved the yield to 85% (ndc) (**Table 2**, entry 3). Although precipitation was reduced compared to the prior Cu(I) strategy, it remained present under these conditions. The optimal outcome (41% yield, ndc; entry 9)**(Table 2)** was achieved by doubling the ethinylestradiol equivalents relative to the fluorinated synthon, using 30 eq. of $CuSO_4$, 100 eq. of sodium ascorbate, and 30 min at 80 °C.

Table 2. Optimization of Huisgen reaction conditions using $CuSO_4$.

Experiment No.	D (equiv)	Ethinylestradiol (equiv)	$CuSO_4$ (0.45 M, equiv)	Ascorbic Acid (1.5 M, equiv)	Reaction Time (min)	Isolated Yield (%)
1	1	6	9	30	15	5.7
2	1	6	30	300	15	54.8
3	1	6	30	300	30	84.8
4	1	2	30	300	15	35.3
5	1	2	30	300	30	73.0
6	1	2	30	30	15	3.8

7	1	2	30	30	30	6.2
8	1	2	30	100	15	15.2
9	1	2	30	100	30	41.2
10	1	2	30	50	15	20.1
11	1	2	30	50	30	41.7

eq = equivalents, Observations: Precipitation was observed in all tested conditions except entry 9 (highlighted in bold).

Figure 7a displays the chromatographic profile for the conditions of **Table 2** entry 9. The main peak at 10.3 min corresponds to [18F]F-FEET, with an impurity at 6.7 min attributed to unreacted D and free fluoride at 2.6 min. Purification via solid-phase extraction on a Sep-Pak® (Waters, Germany) C18 Plus light cartridge yielded a single peak with radiochemical purity (RCP) > 90% at 10.3 min retention time **(Figure 7b).**

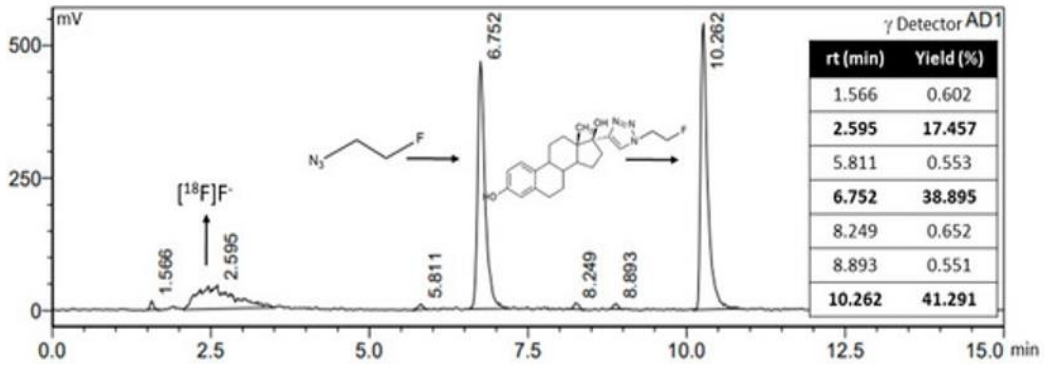

a)

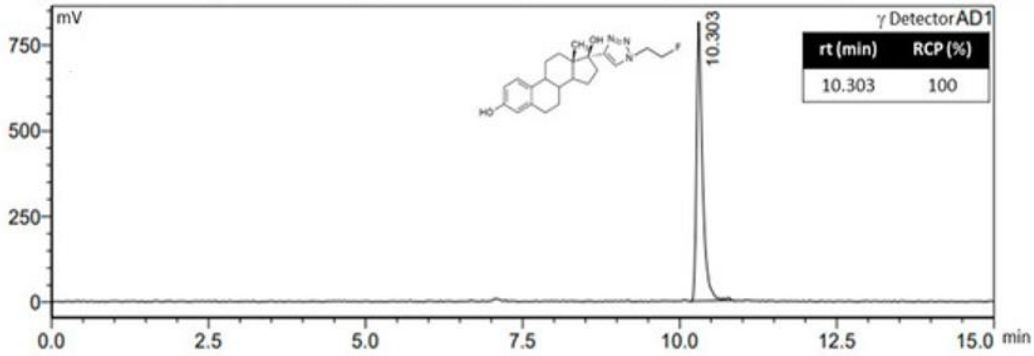

b)

Figure 7. (a) Chromatographic profile obtained for entry 9 of **Table 2**; (b) Chromatographic profile obtained after the purification of [18F]F-FEET.

Complete synthesis of [18F]F-FEET in an automated module

Fully automated production of [18F]F-FEET was accomplished on the Synthra RNplus Research module in 80 min, starting from 3330–3700 MBq activity. As illustrated in **Figure 8,** the process begins with precursor B, where the tosylate is displaced by [18F]fluoride in reactor 1 to form D. The intermediate solution is then transferred to reactor 2 for the Huisgen cycloaddition, yielding [18F]F-FEET. Final purification was carried out within the module using a Sep-Pak® C18 Plus light cartridge (Waters, Germany). The formulated product was passed through a sterile filter, and quality control by HPLC consistently showed a single peak at 10.3 min with 100% RCP.

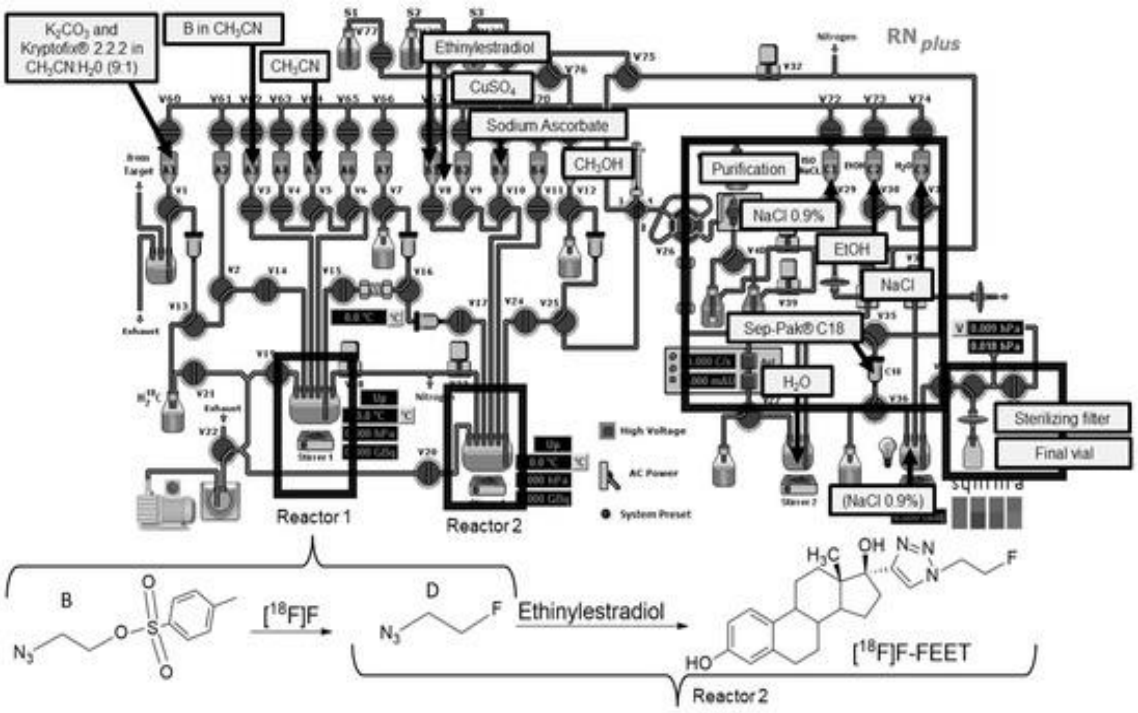

Figure 8. Complete synthesis of [18F]F-FEET in an automated module Synthra RNplus.

Physicochemical studies

Purified [18F]F-FEET underwent evaluation of stability in formulation medium, stability in human serum, lipophilicity, and plasma protein binding (PPB) **(Table 3)** [13].

Table 3. Physicochemical studies of [18F]F-FEET.

Property	Value
Radiochemical purity (RCP) in labeling medium after 4 hours	> 95%
Radiochemical purity (RCP) in human plasma after 4 hours	> 95%
Log P (octanol/aqueous)	1.8 ± 0.1
Plasma protein binding (PPB)	58 ± 7 %

n = 3.

Stability in the labeling medium was assessed by monitoring RCP via HPLC over 4 h post-synthesis, remaining >95% throughout. Serum stability was examined by incubating the radiotracer in human plasma at 37 °C, precipitating proteins, and analyzing the supernatant by HPLC at various time points; this measures only the unbound fraction. [18F]F-FEET maintained RCP >95% for the full 4 h period.

Lipophilicity, expressed as the octanol/phosphate buffer (0.1 M, pH 7.4) partition coefficient, was 1.8 ± 0.1. Plasma protein binding, determined by size-exclusion chromatography, was 58 ± 7%.

In vitro biological studies

In vitro experiments were performed using the MCF-7 cell line (ATCC® HTB-22™, Manassas, VA, USA) [43]. Cellular uptake of [18F]F-FEET was measured at varying tracer activities (0.37, 0.74, 1.85, 3.7 MBq) after 1 h incubation at 37 °C in 5% CO_2 **(Table 4).**

Table 4. Uptake of [18F]F-FEET in MCF-7 cells using different activities of the radiotracer.

(MBq)	% Uptake
0.37	1.0 ± 0.2
0.74	1.3 ± 0.4
1.85	1.3 ± 0.2
3.7	1.0 ± 0.2

n = 3/1 h incubation.

Uptake was also evaluated as a function of incubation time (30, 60, and 120 min) at a fixed activity of 0.74 MBq **(Table 5).** Data from both tables indicate that uptake is largely independent of radiotracer activity and incubation duration within the ranges examined [13,14,44].

Table 5. Uptake of [18F]F-FEET in MCF-7 cells determined at different incubation times.

	% Uptake
30 min	0.60 ± 0.04
1 h	0.6 ± 0.1
2 h	1.0 ± 0.5

n = 3/0.74 MBq.

The preparation of the estradiol-based compound [18F]F-FEET through click chemistry involved nucleophilic substitution via both direct and indirect radiofluorination strategies. The initial approach followed a conventional route, performing radiofluorination directly on the pre-synthesized precursor C, which incorporates the estradiol framework and a tosylate as an effective leaving group for reaction with 18F.

Precursor C was constructed over three steps. The sequence started with replacement of the bromide in commercially available 2-bromoethanol with an azide using NaN_3 in DMSO. Next, the tosylate was introduced employing methylsulfonyl chloride under basic conditions in CH_2Cl_2 as solvent. The final step comprised a Huisgen cycloaddition between the azide of intermediate B and the terminal alkyne of ethinylestradiol. All intermediates were characterized by ^1H NMR. Although the spectrum of C revealed minor contamination by residual ethinylestradiol, its formation was confirmed by a distinctive singlet at δ = 7.52 ppm—absent in ethinylestradiol and assigned to the triazole proton based on literature and prior laboratory findings [13, 14]—verifying successful click conjugation. The remaining proton signals further supported the structure of C.

Direct radiofluorination of C at 90 °C produced [18F]F-FEET in extremely low yield. Evidence of precursor decomposition under these harsh conditions, generating multiple unidentified byproducts, necessitated an alternative strategy to introduce 18F while preserving the structural integrity of the estradiol scaffold.

In radiopharmaceutical synthesis, radionuclides are typically incorporated as the last step. However, when the targeting biomolecule is sensitive, labeling a small prosthetic group first—followed by mild conjugation—is preferred [5, 6].

Numerous prosthetic groups have been described for this purpose, but those equipped with either an azide or alkyne functionality are particularly advantageous owing to the high reliability and selectivity of click cycloadditions. Moreover, the robustness and modular nature of these reactions make them highly suitable for automated platforms commonly employed with positron emitters [5, 6, 45]. Automated synthesizers ensure consistent, reproducible radiopharmaceutical production, minimize operator radiation exposure, and facilitate compliance with good manufacturing practices (GMP) when required. A key limitation, however, is the incompatibility of precipitates with narrow tubing and valves in these modules, which can cause blockages. Thus, adapting click chemistry for automation requires conditions that balance satisfactory radiochemical yield with complete solubility of all components.

While numerous reports describe 18F click reactions in automated systems, automation is frequently limited to prosthetic group radiolabeling, with subsequent biomolecule conjugation performed manually [6].

In contrast, this study reports a fully automated protocol for synthesizing the target radiotracer. Manual optimization of the click conjugation between the prosthetic group and ethinylestradiol preceded transfer to the automated platform.

Click reactions generally proceed via two catalytic systems: direct use of CuI or in situ generation of Cu(I) from Cu(II) salts and sodium ascorbate in aqueous media. We initially explored the CuI route, identifying conditions that delivered good yields but invariably produced precipitates unsuitable for automation. Switching to the more soluble $CuSO_4$ system, combined with methanol to aid dissolution of ethinylestradiol at 80 °C, eliminated precipitation and afforded an overall yield of 41%.

These optimized parameters were successfully implemented in the Synthra RNplus Research module for end-to-end synthesis of [18F]F-FEET while retaining comparable yield.

Fully automated 18F click chemistry remains rare in the literature. One example is the work of Iannone *et al*. [46], who radiolabeled a distinct prosthetic group and coupled it to a novel PSMA-617 analog using Cu(II) salts and sodium ascorbate. Their extensive optimization—driven by the extreme insolubility of the biomolecule—relied

on aqueous-organic solvent mixtures to prevent precipitation, similar to our approach, yet achieved only 6.1% (ndc) overall yield, substantially lower than reported here.

Another case is that of Zhang *et al*. [47], who prepared [18F]DHMT for reactive oxygen species imaging. They employed the same prosthetic group as in this study (1-azido-2-[18F]fluoroethane) but with reduced radiolabeling efficiency (71–87%, ndc) compared to our >90%. Conjugation utilized the Cu(I)-stabilizing ligand TBTA in a mixed solvent system, yielding 6.9% (ndc) of the final tracer—again below our 40%. These comparisons highlight the challenges of automating such reactions and underscore the ongoing need for process refinement to enable routine clinical application of click-based radiotracers.

Following synthesis, purified [18F]F-FEET was subjected to physicochemical characterization, stability assessments, and in vitro evaluation. The compound remained stable in formulation medium and human plasma for at least 4 h, exhibited lipophilicity suitable for passive membrane permeation [48, 49], and showed moderate plasma protein binding. These properties are appropriate for a candidate ER imaging agent. As a nuclear receptor target, ER requires tracers capable of intracellular entry via passive diffusion in the absence of specific transporters. Plasma protein binding strongly influences pharmacokinetics, typically slowing blood clearance for highly bound compounds. The observed PPB for [18F]F-FEET (58 ± 7%) is elevated but markedly lower than that of the parent ethinylestradiol (98.3 ± 0.6%) reported in the literature [50].

Cell-based biological assessments were performed employing the MCF-7 cellular model [43]. MCF-7 cells are extensively utilized in breast cancer investigations due to their accurate representation of various real-world characteristics of the pathology, notably in estrogen receptor-positive (ER+) subtypes. This model's primary strength lies in its robust ERα levels, closely matching those in the majority of aggressive breast tumors, rendering it indispensable for ERα-focused work [51].

Data from **Tables 3 and 4** reveal minimal cell incorporation rates that remained largely unaffected by radiotracer dose or exposure length. Accumulation of [18F]F-FEET reached only 0.8 ± 0.2%, far below the values for unmodified estradiol (6.6 ± 1.4%) and the established benchmark [18F]FES (6.3 ± 1.3%), all obtained via equivalent protocols [14]. Such outcomes point to the molecular alterations required for radioisotope attachment severely compromising ER interaction and affinity. An analogous compound, [18F]F-FETE from Xu and coworkers [52], likewise displayed limited accumulation in MCF-7 cultures. The shared triazole moiety at estradiol's 17-site in these agents—with [18F]F-FEET bearing a short two-carbon spacer at triazole position 4, versus a longer six-carbon chain with dual ether linkages in [18F]F-FETE—highlights the receptor's stringent structural demands. Even though position 17 is generally considered tolerant of changes based on prior studies, these findings underscore the challenges in crafting viable ER probes. This aligns with longstanding hurdles in ER imaging tracer development, exemplified by the limitations of the sole FDA-authorized agent, [18F]fluoroestradiol ([18F]FES) [32], including marked hepatobiliary excretion [22, 25, 28-31].

Conclusion

This work illustrates the effective use of click cycloaddition to construct a prospective radiopharmaceutical through 18F incorporation. The chosen route entailed radiolabeling a compact prosthetic group first, then attaching the sensitive biomolecule under gentle Huisgen conditions. The full sequence was executed on an automated synthesizer, outperforming the modest yields seen in the handful of analogous published cases. While cellular data ruled out utility as an estrogen receptor probe, the achievement remains noteworthy. Fully automating click processes is notoriously difficult, reflected in the few prior successes. Thus, the robust method developed here provides a practical template for upcoming radiotracers built around fragile biomolecules unable to tolerate the aggressive settings of conventional direct fluorination.

Acknowledgments: None

Conflict of Interest: None

Financial Support: None

Ethics Statement: None

References

1. Kolb, H.C.; Finn, M.G.; Sharpless, K.B. Click Chemistry: Diverse Chemical Function from a Few Good Reactions. Angew. Chem. Int. Ed. **2001**, 40, 2004–2021.
2. Hou, J.; Liu, X.; Shen, J.; Zhao, G.; Wang, P.G. The impact of click chemistry in medicinal chemistry. Expert Opin. Drug Discov. **2012**, 6, 489–501.
3. Jiang, X.; Hao, X.; Jing, L.; Wu, G.; Kang, D.; Liu, X.; Zhan, P. Recent applications of click chemistry in drug discovery. Expert Opin. Drug Discov. **2019**, 14, 779–789.
4. Gawon, Y.; Son, J.; Yoo, J.; Park, C.; Koo, H. Application of click chemistry in nanoparticle modification and its targeted delivery. Biomater. Res. **2018**, 22, 13.
5. Choi, J.Y.; Lee, B.C. Click Reaction: An Applicable Radiolabeling Method for Molecular Imaging. Nucl. Med. Mol. Imaging **2015**, 49, 258–267.
6. Bauer, D.; Cornejo, M.A.; Hoang, T.T.; Lewis, J.J.; Zeglis, B.M. Click Chemistry and Radiochemistry: An Update. Bioconjugate Chem. **2023**, 34, 1925–1950.
7. Mindt, T.L.; Struthers, H.; Brans, L.; Anguelov, T.; Schweinsberg, C.; Maes, V.; Tourwe, D.; Schibli, R. "Click to Chelate": Sythesis and Installation of Metal Chelates into Biomolecules in a Single Step. J. Am. Chem. Soc. **2006**, 128, 15096–15097.
8. Kluba, C.A.; Mindt, T.M. Click-to-Chelate: Development of Technetium and Rhenium-Tricarbonyl Labeled Radiopharmaceutical. Molecules **2013**, 18, 3206–3226.
9. Notni, J.; Wester, H.J. A Practical Guide on the Synthesis of Metal Chelates for Molecular Imaging and Therapy by Means of Click Chemistry. Chem. Eur. J. **2016**, 22, 11500–11508.
10. Ferro-Flores, G.; Rivero, I.; Santos-Cuevas, C.; Sarmiento, J.; Arteaga de Murphy, C.; Ocampo-García, B.; García-Becerra, R.; Ordaz-Rosado, D. Click chemistry for [Tc-99m$(CO)_3$] labeling of Lys(3)-bombesin. Appl. Radiat. Isot. **2010**, 68, 2274–2278.
11. Fernández, S.; Crócamo, N.; Incerti, M.; Giglio, J.; Scarone, L.; Rey, A. Preparation and preliminary bioevaluation of a ^{99m}Tc$(CO)_3$-glucose derivative prepared by a click chemistry route. J. Label. Compd. Radiopharm. **2012**, 55, 274–280.
12. Fernández, S.; Giglio, J.; Rey, A.M.; Cerecetto, H. Influence of ligand denticity on the properties of novel ^{99m}Tc(I)–carbonyl complexes. Application to the development of radiopharmaceuticals for imaging hypoxic tissue. Bioorg. Med. Chem. **2012**, 20, 4040–4048.
13. Tejería, M.E.; Giglio, J.; Dematteis, S.; Rey, A. Development and characterization of a ^{99m}Tc-tricarbonyl–labelled estradiol derivative obtained by "Click Chemistry" with potential application in estrogen receptors imaging. J. Label. Comp. Radiopharm. **2017**, 60, 521–527.
14. Tejería, E.; Giglio, J.; Fernández, L.; Rey, A. Development and evaluation of a ^{99m}Tc(V)-nitrido complex derived from estradiol for breast cancer imaging. Appl. Radiat. Isot. **2019**, 154, 108854.
15. Colibri UdelaR. Available online: **https://www.colibri.udelar.edu.uy/jspui/handle/20.500.12008/32120** (accessed on 15 December 2023).
16. Cardoso, M.E.; Decuadra, P.; Zeni, M.; Delfino, A.; Tejería, M.E.; Coppe, F.; Mesa, J.M.; Daher, G.; Giglio, J.; Carrau, G.; et al. Development and Evaluation of ^{99m}Tc Tricarbonyl Complexes Derived from Flutamide with Affinity for Androgen Receptor. Molecules **2023**, 28, 820.
17. Jacobson, O.; Kiesewetter, D.O.; Chen, X. Fluorine-18 Radiochemistry, Labeling Strategies and Synthetic Routes. Bioconjugate Chem. **2015**, 26, 1–18.
18. Jia, L.; Cheng, Z.; Shi, L.; Li, J.; Wang, C.; Jiang, D.; Zhou, W.; Meng, H.; Qi, Y.; Cheng, D.; et al. Fluorine-18 labeling by click chemistry: Multiple probes in one pot. Appl. Radiat. Isot. **2013**, 75, 64–70.
19. Pretze, M.; Mamat, C. Automated preparation of [^{18}F]AFP and [^{18}F]BFP: Two novel bifunctional ^{18}F-labeling building blocks for Huisgen-click. J. Fluorine Chem. **2013**, 150, 25–35.
20. Cheng, S.; Jacobson, O.; Zhu, G.; Chen, Z.; Liang, S.H.; Tian, R.; Yang, Z.; Niu, G.; Zhu, X.; Chen, X. PET imaging of EGFR expression using an ^{18}F-labeled RNA aptamer. Eur. J. Nucl. Med. Mol. Imaging **2019**, 46, 948–956.
21. van Kruchten, M.; de Vries, E.G.E.; Brown, M.; de Vries, E.F.J.; Glaudemans, A.W.J.M.; Dierckx, R.A.J.O.; Schröder, C.P.; Hospers, G.A.P. PET imaging of estrogen receptors in patients with breast cancer. Lancet Oncol. **2013**, 14, 465–475.

22. François, B.; Mavi, A. Receptor Imaging in Patients with Breast Cancer. PET Clin. **2009**, 4, 329–341.
23. Hanstein, B.; Djahansouzi, S.; Dall, P.; Beckmann, M.W.; Bender, H.G. Insights into the molecular biology of the estrogen receptor define novel therapeutic targets for breast cancer. Eur. J. Endocrinol. **2004**, 150, 243–255.
24. Sommer, S.; Fuqua, S.A.W. Estrogen receptor and breast cancer. Semin. Cancer Biol. **2001**, 11, 339–352.
25. Kurdziel, K.A.; Ravizzini, G.; Croft, B.Y.; Tatum, J.L.; Choyke, P.L.; Kobayashi, H. The evolving role of nuclear molecular imaging in cancer. Expert Opin. Med. Diagn. **2008**, 7, 829–842.
26. Kiesewetter, D.O.; Kilbourn, M.R.; Landvatter, S.W.; Heiman, D.F.; Katzenellenbogen, J.A.; Welch, M.J. Preparation of four fluorine-18-labeled estrogens and their selective uptakes in target tissues of immature rats. J. Nucl. Med. **1984**, 25, 1212–1221.
27. Scott, P.J.H.; Hockley, B.G. Radiochemical Syntheses: Radiopharmaceuticals for Positron Emission Tomography; Wiley: Hoboken, NJ, USA, 2011; Volume 1, pp. 69–80.
28. Mintun, M.A.; Welch, M.J.; Siegel, B.A.; Mathias, C.J.; James, M.S.S.; Brodack, W.; McGuire, A.H.; Katzenellenbogen, J.A. Breast Cancer: PET Imaging of Estrogen Receptors. Radiology **1988**, 69, 45–48.
29. Sundararajan, L.; Linden, H.M.; Link, J.M.; Krohn, K.A.; Mankoff, D.A. ^{18}F-Fluoroestradiol. Semin. Nucl. Med. **2007**, 37, 470–476.
30. Eckelman, W. The Application of Receptor Theory to Receptor-binding and Enzyme-binding Oncologic Radiopharmaceuticals. Nucl. Med. Biol. **1994**, 21, 759–769.
31. Heesch, A.; Maurer, J.; Stickeler, E.; Beheshti, M.; Mottaghy, F.M.; Morgenroth, A. Development of Radiotracers for Breast Cancer—The Tumor Microenvironment as an Emerging Target. Cells **2020**, 9, 2334.
32. ZIONEXA. Available online: **https://www.zionexa.com/2020/05/27/zionexa-usa-and-petnet-solutions-announce-fdaapproval-of-cerianna-fluoroestradiol-f18/** (accessed on 15 December 2023).
33. Brzozowski, A.M.; Pike, A.C.W.; Dauter, Z.; Hubbard, R.E.; Bonn, T.; Engström, O.; Öhman, L.; Greene, G.; Gustafsson, J.; Carlquist, M. Molecular basis of agonism and antagonism in the oestrogen receptor. Nature **1997**, 389, 753–758.
34. Dessislava, J.; Frateva, F.; Tsakovska, I.; Alova, P.; Pencheva, T.; Pajeva, I. Molecular dynamics simulation of the human estrogen receptor alpha: Contribution to the pharmacophore of the agonists. Math. Comput. Simul. **2015**, 133, 124–134.
35. Kreimerman, I.; Porcal, W.; Olivera, S.; Oliver, P.; Savio, E.; Engler, H. Synthesis of [^{18}F]2B-SRF101: A Sulfonamide Derivative of the Fluorescent Dye Sulforhodamine 101. Curr. Radiopharm. **2017**, 10, 212–220.
36. Berta, M.; Dancsó, A.; Nemes, A.; Pathó, Z.; Szabó, D.; Rábai, J. Convenient Synthesis of Pure Fluorous Alkyl Azides at Multigram Scale. J. Fluor. Chem. **2016**, 16, 30240–30248.
37. Hay, M.P.; Wilson, W.R.; Moselen, J.W.; Palmer, B.D.; Denny, W.A. Hypoxia-Selective Antitumor Agents. 8. Bis(nitroimidazoly1)alkanecarboxamides: A New Class of Hypoxia-Selective Cytotoxins and Hypoxic Cell Radiosensitisers. J. Med. Chem. **1994**, 37, 381–391.
38. Pereira, M.P.; Tejería, M.E.; Zeni, M.; Gambini, J.P.; Duarte, P.; Rey, A.; Giglio, J. Radiosynthesis and validation of [^{18}F]fluoroestradiol in a Synthra plus research platform for use in routine clinical practic. J. Label. Comp. Radiopharm. **2022**, 65, 292–297.
39. Hausner, S.H.; Marik, J.; Gagnon, M.K.J.; Sutcliffe, J.L. In Vivo Positron Emission Tomography (PET) Imaging with an $\alpha_v\beta_6$ Specific Peptide Radiolabeled using ^{18}F-"Click" Chemistry: Evaluation and Comparison with the Corresponding 4-[^{18}F]Fluorobenzoyl- and 2-[^{18}F]Fluoropropionyl-Peptides. J. Med. Chem. **2008**, 51, 5901–5904.
40. Marik, J.; Sutcliffe, J.L. Click for PET: Rapid preparation of [^{18}F]fluoropeptides using CuI catalyzed 1,3-dipolar cycloaddition. Tetrahedron Lett. **2006**, 47, 6681–6684.
41. Evans, H.L.; Carroll, L.; Aboagye, E.O.; Spivey, A.C. Bioorthogonal chemistry for ^{68}Ga radiolabeling of DOTA-containing compounds. J. Label. Comp. Radiopharm. **2014**, 57, 291–297.
42. Glaser, M.; Arstad, E. "Click Labeling" with 2-[^{18}F]Fluoroethylazide for Positron Emission Tomography. Bioconjugate Chem. **2007**, 18, 989–993.
43. ATCC. Available online: **https://www.atcc.org/Products/All/HTB-22.aspx#characteristics** (accessed on 15 December 2023).
44. Xia, X.; Feng, H.; Li, C.; Qin, C.; Song, Y.; Zhang, Y.; Lan, X. ^{99m}Tc-labeled estradiol as an estrogen receptor probe: Preparation and preclinical evaluation. Nucl. Med. Biol. **2016**, 43, 89–96.

45. Banister, S.; Roeda, D.; Dolle, D.; Kassiou, M. Fluorine 18- Chemistry for PET: A concise introduction. Curr. Radiopharm. **2010**, 3, 68–80.
46. Iannone, M.N.; Stucchi, S.; Turolla, E.A.; Beretta, C.; Ciceri, S.; Chinello, C.; Pagani, L.; Todde, S.; Ferraboschi, P. Synthesis and automated fluorine-18 radiolabeling of new PSMA-617 derivatives with a CuAAC radiosynthetic approach. J. Label. Compd. Radiopharm. **2021**, 65, 48–62.
47. Zhang, W.; Cai, Z.; Li, L.; Ropchan, J.; Lim, K.; Boutagy, N.E.; Wu, J.; Stendahl, J.C.; Chu, W.; Gropler, R.; et al. Optimized and Automated Radiosynthesis of [^{18}F]DHMT for Translational Imaging of Reactive Oxygen Species with Positron Emission Tomography. Molecules **2016**, 21, 1696.
48. Liu, X.; Testa, B.; Fahr, A. Lipophilicity and Its Relationship with Passive Drug Permeation. Pharm. Res. **2011**, 28, 962–977.
49. Arnott, J.A.; Planey, S.L. The influence of lipophilicity in drug discovery and design. Expert Opin. Drug Discov. **2012**, 7, 909–921.
50. Estradiol Catalog NoS1709 Selleckchem. Houston, Texas. Available online: **http://www.selleckchem.com/datasheet/Estradiol-DataSheet.html** (accessed on 2 February 2024).
51. Freshney, R.I. Culture of Animal Cells: A Manual of Basic Technique; John Wiley and Sons, Inc.: Hoboken, NJ, USA, 2005.
52. Xu, D.; Zhuang, R.; You, L.; Guo, Z.; Wang, X.; Peng, C.; Zhang, D.; Zhang, P.; Wu, H.; Pan, W.; et al. ^{18}F–labeled estradiol derivative for targeting estrogen receptor-expressing breast cancer. Nucl. Med. Biol. **2018**, 59, 48–55.